J|A|C|S ARTICLES

Published on Web 02/05/2010

Editing Mechanism of Aminoacyl-tRNA Synthetases Operates by a Hybrid Ribozyme/Protein Catalyst

Yohsuke Hagiwara,[†,‡] Martin J. Field,[§] Osamu Nureki,[||] and Masaru Tateno*[,†,‡]

Center for Computational Sciences, University of Tsukuba, Tennodai 1-1-1, Tsukuba Science City, Ibaraki 305-8577, Japan, Graduate School of Pure and Applied Sciences, University of Tsukuba, Tennodai 1-1-1, Tsukuba, Ibaraki 305-8571, Japan, Laboratoire de Dynamique Moléculaire, Insitut de Biologie Structurale Jean-Pierre Ebel, 41 rue Jules Horowitz, 38027 Grenoble Cedex 1, France, and Institute of Medical Science, University of Tokyo, Shirokanedai 4-6-1, Minatoku, Tokyo 108-8639, Japan

Received November 9, 2009; E-mail: tateno@ccs.tsukuba.ac.jp

Abstract: Aminoacyl-tRNA synthetases (aaRSs) are critical for the translational process, catalyzing the attachment of specific amino acids to their cognate tRNAs. To ensure formation of the correct aminoacyl-tRNA, and thereby enhance the reliability of translation, several aaRSs have an editing capability that hinders formation of misaminoacylated tRNAs. We investigated theoretically the mechanism of the editing reaction for a class I enzyme, leucyl-tRNA synthetase (LeuRS), complexed with a misaminoacylated $tRNA^{Leu}$, employing ab initio hybrid quantum mechanical/molecular mechanical potentials in conjunction with molecular dynamics simulations. It is shown that the water molecule that acts as the nucleophile in the editing reaction is activated by a 3′-hydroxyl group at the 3′-end of $tRNA^{Leu}$ and that the O2′ atom of the leaving group of the substrate is capped by one of the water's hydrogen atoms. Thus, it is shown that editing is a self-cleavage reaction of the tRNA and so it is the tRNA, and not the protein, that drives the reaction. The protein does, however, have an important stabilizing effect on some high-energy intermediates along the reaction path, which is more efficient than the ribozyme would be alone. This indicates that editing is achieved by a novel "hybrid ribozyme/protein catalyst". Analysis of existing experimental data and additional modeling shows that this ribozymal mechanism appears to be widespread, occurring in the ribosome as well as in other aaRSs. It also suggests transitional forms that could have played an important role in the RNA world hypothesis for the origin of life.

1. Introduction

Aminoacyl-tRNA synthetases (aaRSs) are responsible for linking their cognate amino acid to the 3′-end of specific tRNAs. This aminoacylation proceeds in two steps: first, the amino acid is activated by ATP to the aminoacyl adenylate with liberation of pyrophosphate, and second, the amino acid moiety of the aminoacyl adenylate is transferred to the 3′-end of the tRNA. aaRSs are classified into two families of 10 enzymes each, classes I and II.[1,2] Class I enzymes have a catalytic core based on the classical nucleotide-binding fold (Rossmann fold), whereas the active sites of class II enzymes contain an antiparallel β sheet flanked by α helices. The fidelity of translation, and thus the accurate conversion of genetic information, depends in large part on the specificity with which amino acids are attached to their cognate tRNAs. However, the coexistence of chemically and structurally similar amino acids can make it difficult for aaRSs to distinguish their cognate amino acids from noncognate ones. To overcome this problem, the following aaRSs employ a "double sieve" editing mechanism: class Ia, leucyl (LeuRS), isoleucyl (IleRS), valyl (ValRS); class IIa, threonyl (ThrRS) and alanyl (AlaRS); and class IIc, phenylananyl (PheRS).[3−10] The first sieve, which acts at the aminoacylation site, is coarse, and its role is to exclude amino acid molecules that are larger than the cognate amino acid or those that cannot establish specific interactions. After this stage, the activation and attachment of amino acids to tRNAs is possible. The second sieve is a fine one and catalyzes the hydrolysis of the misactivated or misacylated products of activation or attachment. This reaction is achieved at an editing

[†] Center for Computational Sciences, University of Tsukuba.
[‡] Graduate School of Pure and Applied Sciences, University of Tsukuba.
[§] Insitut de Biologie Structurale Jean-Pierre Ebel.
[||] University of Tokyo.

(1) Cusack, S.; Berthet-Colominas, C.; Hartlein, M.; Nassar, N.; Leberman, R. *Nature* **1990**, *347*, 249–55.
(2) Eriani, G.; Delarue, M.; Poch, O.; Gangloff, J.; Moras, D. *Nature* **1990**, *347*, 203–6.
(3) Fukai, S.; Nureki, O.; Sekine, S.; Shimada, A.; Tao, J.; Vassylyev, D. G.; Yokoyama, S. *Cell* **2000**, *103*, 793–803.
(4) Fukunaga, R.; Fukai, S.; Ishitani, R.; Nureki, O.; Yokoyama, S. *J. Biol. Chem.* **2004**, *279*, 8396–402.
(5) Fukunaga, R.; Yokoyama, S. *J. Biol. Chem.* **2005**, *280*, 29937–45.
(6) Lincecum, T. L., Jr.; Tukalo, M.; Yaremchuk, A.; Mursinna, R. S.; Williams, A. M.; Sproat, B. S.; Van Den Eynde, W.; Link, A.; Van Calenbergh, S.; Grotli, M.; Martinis, S. A.; Cusack, S. *Mol. Cell* **2003**, *11*, 951–63.
(7) Mursinna, R. S.; Lincecum, T. L., Jr.; Martinis, S. A. *Biochemistry* **2001**, *40*, 5376–81.
(8) Nureki, O.; Vassylyev, D. G.; Tateno, M.; Shimada, A.; Nakama, T.; Fukai, S.; Konno, M.; Hendrickson, T. L.; Schimmel, P.; Yokoyama, S. *Science* **1998**, *280*, 578–82.
(9) Silvian, L. F.; Wang, J.; Steitz, T. A. *Science* **1999**, *285*, 1074–7.
(10) Zhai, Y.; Martinis, S. A. *Biochemistry* **2005**, *44*, 15437–43.

Table 1. Summary of the QM/MM MD Simulations Used To Obtain the PESs

simulation	purpose	initial state	figure [a]	reaction coordinate	windows	variable range
1	testing of scheme 1	state 1	S3A	O_w-C	20	3.4 → 1.5 Å
				$O^{2'}-C$	15	1.3 → 1.5 Å
2	testing of scheme 2	state 1	S3B	$O_w-C + H_w-O^{2'}$	47	7.0 → 2.4 Å
3	testing of scheme 1	state 3	2A left	O_w-C	10	2.4 → 1.5 Å
				$O^{2'}-C$	12	1.3 → 1.8 Å
			2A right	$H_{w2}-O^{2'}$	17	2.5 → 0.9 Å
				$O^{2'}-C$	18	1.3 → 3.0 Å
			S6	$H_{w1}-O^{2'}$	17	2.5 → 0.9 Å
				$O^{2'}-C$	12	1.3 → 2.4 Å
4	testing of scheme 2	state 3	S3C	$H_w-O^{2'}$	17	2.5 → 0.9 Å
				$O^{2'}-C$	15	1.3 → 1.5 Å
			S3D	O_w-C	8	2.2 → 0.9 Å
				$O^{2'}-C$	16	1.5 → 3.0 Å
5	rotation of 3′-HO	state 1	S4	$C^{2'}-C^{3'}-O^{3'}-3'HO$	16	50° → 200°
6	transition from state 2 to state 3	state 2	S5	O_w-C	11	3.4 → 2.4 Å

[a] Figures with an "S" prefix are in the Supporting Information.

site which is too small to accommodate the cognate amino acid, but can fit the noncognate ones that permeate the first sieve.

Two distinct possibilities exist for second-sieve hydrolysis. In pretransfer editing, a misactivated amino acid is hydrolyzed to the amino acid and AMP, whereas in post-transfer editing a misaminoacylated tRNA is hydrolyzed to the amino acid and tRNA. *Thermus thermophilus* LeuRS is currently the only system for which the crystal structures of the two distinct complexes have been reported. One is the complex with an inhibitor of the pretransfer editing, 5′-*O*-[*N*-(L-norvalyl)sulfamoyl]adenosine, and the other is the complex with $tRNA^{Leu}$, in which the 3′-terminus is bound to the editing site, but the misaminoacylated amino acid moiety is absent. Nevertheless, for most eubacterial LeuRSs, pretransfer editing activity has not been detected, whereas post-transfer editing has been confirmed.[6,7,10]

The substrate of the post-transfer reaction contains a labile ester linkage between $O^{2'}$ or $O^{3'}$ of the 3′-end nucleotide (adenine-76; A76) of tRNA and the carbonyl carbon of its amino acid moiety and it is the latter carbon atom that is supposed to be attacked by a nucleophile in the hydrolysis. Experimental investigations of variants of tRNAs, in which 2′ or 3′ hydroxyl (OH) groups of A76 are removed, have revealed a difference in behavior among the class Ia aaRSs, as in LeuRS the rate of editing activity is significantly reduced, whereas it is much less affected in the other two systems, IleRS and ValRS (see the Supporting Information, section S1).[11] Thus, the details of the post-transfer editing reaction have yet to be elucidated experimentally.

In this study, we have explored possible reaction mechanisms for post-transfer editing in class Ia aaRS. Most work was done on LeuRS complexed with misaminoacylated $tRNA^{Leu}$, but IleRS and ValRS were also modeled. We employed hybrid quantum mechanical (QM)/molecular mechanical (MM) potentials with all-electron ab initio density functional theory QM methods, in conjunction with molecular dynamics (MD) simulations, to calculate the potential energy surfaces (PESs) for the various hypotheses. This is a state-of-the-art theoretical methodology for investigating reaction mechanisms in large systems such as biological macromolecules. A full summary of the QM/MM MD simulations that we performed is given in Table 1.

(11) Nordin, B. E.; Schimmel, P. *Biochemistry* **2003**, *42*, 12989–97.

2. Materials and Methods

2.1. System Preparation. The initial coordinates were taken from the crystal structure of the complex of the *T. thermophilus* leucyl-tRNA synthetase (LeuRS) and $tRNA^{Leu}$ (accession code 2BYT in the Protein Data Bank). In this crystal structure, the valine moiety attached to A76 and structural water molecules, which are essential for the editing reaction, are absent. Accordingly, to construct the modeled structure of the fully solvated LeuRS complexed with misaminoacylated $tRNA^{Leu}$, we developed a novel scheme that couples molecular docking and molecular dynamics (MD) simulations.[12] The final model system comprised 165 739 atoms and included 49 587 water molecules.

MD simulations were performed using the AMBER 8 program with use of the parm99 force field.[13] The TIP3P model was used for solvent water molecules. Periodic boundary conditions were employed and all electrostatic interactions were calculated using a particle-mesh Ewald (PME) method with a dielectric constant of unity.[14] A 12 Å cutoff was used to calculate the direct space sum for PME, and electrostatic interactions beyond 12 Å were calculated in reciprocal space by fast Fourier transform. The SHAKE algorithm was used to restrain bond lengths involving hydrogen atoms.[15] The time step for integration was set to 1 fs. The temperature and pressure were maintained at 300 K and 1 atm using the Berendsen algorithm.[16]

2.2. QM/MM Hybrid MD Simulations. Initially we performed a 1-ns MD simulation for the LeuRS·valyl-$tRNA^{Leu}$ complex to equilibrate the system and obtained the structure of the complex defined as state 1.[17] For the MD simulations with the hybrid quantum mechanical (QM)/molecular mechanical (MM) potential, the following atoms were assigned as QM atoms: the valine and ribose moieties of the substrate and the groups that hydrogen bond with them, i.e., two water molecules (referred to as W_1 and W_2), Thr247, Thr248, and the side chain of Asp347. In all, there were 77 atoms, including hydrogen link atoms, in the QM region. For the MD simulations the integration time step was reduced to 0.1 fs. The programs used for the QM/MM MD simulations were

(12) Hagiwara, Y.; Nureki, O.; Tateno, M. *FEBS Lett.* **2009**, *583*, 825–830.
(13) Case, D. A.; Cheatham, T. E.; Darden, T.; Gohlke, H.; Luo, R.; Merz, K. M.; Onufriev, A.; Simmerling, C.; Wang, B.; Woods, R. J. *J. Comput. Chem.* **2005**, *26*, 1668–88.
(14) Darden, T.; York, D.; Pedersen, L. *J. Chem. Phys.* **1993**, *98*, 10089–92.
(15) Ryckaert, J. P.; Ciccotti, G.; Berendsen, H. J. C. *J. Comput. Phys.* **1977**, *23*, 327–41.
(16) Berendsen, H. J. C.; Postma, J. P. M.; Vangunsteren, W. F.; Dinola, A.; Haak, J. R. *J. Chem. Phys.* **1984**, *81*, 3684–90.
(17) Hagiwara, Y.; Nureki, O.; Tateno, M. *FEBS Lett.* **2009**, *583*, 1901–8.

GAMESS,[18] AMBER,[13] and our interface program that connects these two engines.[19] Calculations for the atoms in the QM region were done with an all-electron spin-restricted density functional theory (DFT) method employing the B3LYP hybrid functional[20,21] and the 6-31G* basis set.

The link atom approach[22] was used to treat covalent bonds between atoms of the QM and MM regions. Calculations of the electrostatic interactions between QM and MM atoms were carried out with a dual approach in which the partial charges of MM atoms within 25 Å of the center of mass of the QM region were incorporated into the one-electron integral term in the QM Hamiltonian, whereas the remainder were evaluated at the MM level. Partial charges for the QM atoms were taken from the AMBER force field.

The energy surfaces for the various mechanistic hypotheses that we investigated were obtained as functions of sets of predefined reaction coordinate variables. We employed an adiabatic mapping approach, based upon geometry optimization, but augmented with MD simulations to enhance conformational sampling. Thus, we divided the reaction space into windows, each defined by a particular set of values of the reaction coordinate variables, and then, for each window, performed a short MD simulation followed by a geometry optimization. Both the MD simulations and geometry optimizations were carried out with functions that constrained the reaction coordinate variables to remain close to their window reference values. The final potential energy surfaces (PESs) were then reconstructed from the energies of the geometry-optimized structures but without the constraint energy terms.

To characterize the transition states, identified as the structures of highest potential energy along the PES, we performed DFT normal-mode analyses of isolated models of the structures corresponding to the QM region employing the B3LYP functional and the 6-31G* basis set. Finally, the energy profiles were redetermined via single-point energy calculations of the DFT-optimized structures using a Møller−Plesset second order perturbation (MP2) method[23] with the larger 6-31+G** basis set.

A full summary of the QM/MM MD simulations that we performed is given in Table 1. One-dimensional (1D) profiles or two-dimensional (2D) surfaces were determined, depending upon the reaction step being investigated. The optimized structures corresponding to states 1 and 3 were the initial structures for the QM/MM MD simulations performed in the present study and, for each of them, two reaction schemes were investigated. Thus, four sets of QM/MM MD simulations were performed to obtain the energy landscapes of the reactions, which we refer to as simulations 1−4. For the rotation of the 3′-HO group from state 1 and the structural transition from state 2 to state 3, further simulations were carried out. These are referred to as simulations 5 and 6, respectively.

Harmonic constraint potentials were employed for most reaction coordinate variables with force constants of 200 kcal/mol and updating every 100 simulation steps. A constraint function was found to be unnecessary for the $O^{2'}-C$ distance in simulations when this was a variable, since its value naturally increased and was adequately sampled, as a result of the nucleophilic attack occurring in the MD simulations.

(18) Schmidt, M. W.; Baldridge, K. K.; Boatz, J. A.; Elbert, S. T.; Gordon, M. S.; Jensen, J. H.; Koseki, S.; Matsunaga, N.; Nguyen, K. A.; Su, S. J.; Windus, T. L.; Dupuis, M.; Montgomery, J. A. *J. Comput. Chem.* **1993**, *14*, 1347–1363.
(19) Ohta, T.; Hagiwara, T.; Kang, J.; Nishikawa, K.; Yamamoto, T.; Nagao, H.; Tateno, M. *J. Comp. Theor. Nanosci.* **2009**, *6*, 2648–55.
(20) Becke, A. D. *J. Chem. Phys.* **1993**, *98*, 5648–52.
(21) Lee, C. T.; Yang, W. T.; Parr, R. G. *Phys. Rev. B* **1988**, *37*, 785–9.
(22) Field, M. J.; Bash, P. A.; Karplus, M. *J. Comput. Chem.* **1990**, *11*, 700–33.
(23) Headgordon, M.; Pople, J. A.; Frisch, M. J. *Chem. Phys. Lett.* **1988**, *153*, 503–6.

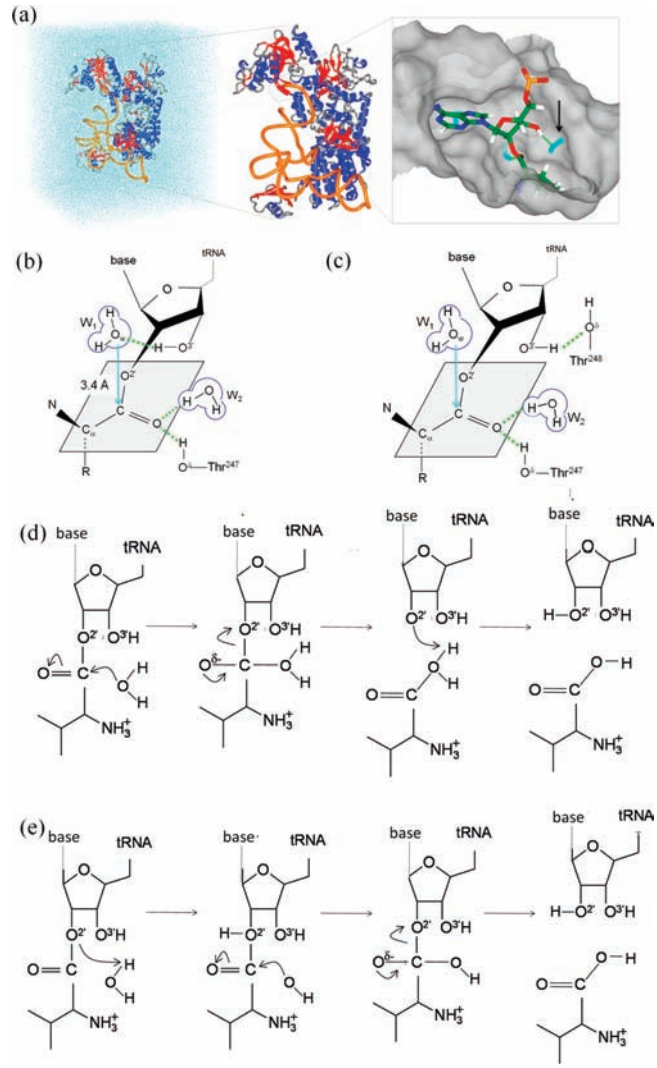

Figure 1. The entire system studied in the present work is depicted, and possible reaction mechanisms of editing are shown. (a) The left panel shows the overall system used in the QM/MM MD simulations. The middle panel represents the three-dimensional (3D) structure of the LeuRS·valyl-$tRNA^{Leu}$ complex, and the right panel shows valine-attached A76, the nucleophilic water, and the molecular surface of the catalytic site of LeuRS. The backbone of $tRNA^{Leu}$ is shown in a tube representation (orange). The water acting as the nucleophile is marked by black arrows. (b and c) Schematic representation of states 1 (B) and 2 (C) and the corresponding 3-D structures taken from the MD simulation. (d) The mechanism, scheme 1, initiated by attack of nucleophilic water and bond formation between the C and O_w atoms. (e) The mechanism, scheme 2, initiated by abstraction of the hydrogen atom of the nucleophilic water.

3. Results and Discussion

3.1. Exploration of Reaction Pathways (Part I). In our previous study, a completely solvated structure of the LeuRS·valyl-$tRNA^{Leu}$ complex was constructed (Figure 1a), and two water molecules, W_1 and W_2, were revealed to be located in the vicinity of the carbonyl carbon of the substrate (referred to as the C atom here; Figure 1b).[12] W_1 is hydrogen-bonded to the 3′-hydroxyl group of A76 of $tRNA^{Leu}$ (3′-HO) and is located in an optimum position to act as the nucleophile for hydrolysis, the distance between C and the oxygen atom of W_1 (O_w atom) being 3.4 Å (Figure 1a).[17] The other water molecule, W_2, is hydrogen-bonded to the carbonyl oxygen atom of the substrate (O atom) and that of Phe246. We refer to this structure as state 1 (Figure 1b).

We investigated two mechanisms (schemes 1 and 2) for the editing reaction using state 1 as the initial configuration. In scheme 1 (see the Supporting Information, Figure S1a), the reaction is initiated by bond formation between the C and O_w atoms, followed by cleavage of the $O^{2'}-C$ bond and abstraction of a hydrogen atom of W_1 by the $O^{2'}$ atom. In scheme 2 (see the Supporting Information, Figure S1b), abstraction of the hydrogen atom is considered to occur prior to $C-O_w$ bond formation. To test these schemes, we calculated two-dimensional (2D) PESs via QM/MM MD simulations (referred to as simulations 1 and 2, respectively) and found that energy barriers of 48.2 and 49.6 kcal/mol were required for schemes 1 and 2, respectively (see the Supporting Information, Figures S2, S3a,b). These high barriers suggest that O_w, which attacks the C in scheme 1, and $O^{2'}$, which abstracts the hydrogen in scheme 2, are not sufficiently activated prior to bond formation and imply that these mechanisms, both initiated from state 1, are not feasible (for more detailed discussions, see the Supporting Information, section S2.1).

3.2. Exploration of Reaction Pathways (Part II): The Productive Mechanisms. If the O_w atom is to gain access to the C atom, thereby leading to O_w-C bond formation, rotation of the 3′-HO group is required.[17] To explore this possibility, we performed an additional QM/MM MD simulation of the LeuRS·valyl-$tRNA^{Leu}$ complex and identified a structure in which the 3′-HO is rotated by approximately 80° with respect to that of state 1 (simulation 5). This structure, which we denote state 2 (Figure 1c), is stabilized by a hydrogen bond between 3′-HO and the HO^{δ} atom of Thr248 and is separated from state 1 by an energy barrier of only 4.5 kcal/mol (see the Supporting Information, Figure S4). To investigate the interaction energy between W_1 and the substrate with the rotated 3′-HO group, we calculated a one-dimensional (1D) PES as a function of the O_w-C distance, starting from the state 2 structure (simulation 6). From this, we identified a new structure, state 3 (Figure 2a), of comparable energy to state 2 and separated from it by a small energy barrier of 4.2 kcal/mol (see the Supporting Information, Figure S5). The O_w-C distance in state 3 is 2.4 Å, compared to the 3.4 Å observed in states 1 and 2, and the orientation of the nucleophilic water molecule is changed, as there is a hydrogen bond between $O^{3'}$ and a hydrogen atom of W_1 (this hydrogen atom is referred to as H_{w1} and the other hydrogen atom of W_1 as H_{w2}; Figure 2a). State 3 appeared as a more suitable starting point for the editing reaction, so we re-examined schemes 1 and 2 initiated from it by means of QM/MM MD simulations (Figure 1d,e).

3.3. Activation of the Nucleophilic Water through the Formation of a Low-Barrier Hydrogen Bond with the 3′-HO of A76 of $tRNA^{Leu}$. To investigate the plausibility of scheme 1 (Figure 1d), we calculated a 2D PES using the $C-O_w$ and $O^{2'}-C$ distances as reaction coordinates (simulation 3) (Figure 2a). The evolution of atomic distances during the MD simulation shows that $C-O_w$ bond formation is followed by elongation of the $O^{2'}-C$ bond as the $C-O^{2'}$ distance only begins to increase when the $C-O_w$ distance decreases below 1.8 Å (state 4) (Figure 2b). The maximum energy, 23.2 kcal/mol, is observed when the $C-O_w$ distance reaches 1.6 Å (state 5) (Figure 2a). Normal mode analysis confirmed that this structure was a saddle point for the reaction, with a single imaginary frequency involving the reacting atoms, whose high energy can be attributed to the elongation of the $O^{2'}-C$ covalent bond from ∼1.4 to ∼1.6 Å (Figure 2b). Subsequently, a metastable state, state 6 (Figure 2a), is formed that is 19.8 kcal/mol higher in energy than state 3. This occurs by further elongation of the $O^{2'}-C$ covalent bond, together with a dramatic decrease in the $O^{3'}-H_{w1}$ distance (Figure 2b). This behavior is reminiscent of the presence of a low-barrier hydrogen bond (LBHB). These have been identified in various systems via high-resolution X-ray and neutron crystallography and have been shown to play a critical role in activating nucleophiles and/or stabilizing transition states in three enzymatic reactions (see the Supporting Information, Figure S7, section S3). The formation of a LBHB between the 3′-OH of A76 and the nucleophile accelerates the reaction by compensating for the increase in energy induced by elongation of the $O^{2'}-C$ bond.

3.4. Stabilization of High-Energy Intermediates through Hydrogen-Bond Networks between LeuRS and $tRNA^{Leu}$. The 3′-HO and $O^{3'}$ atoms in these states form hydrogen bonds with the O^{δ} atom and the amide hydrogen of Thr248, respectively. This hydrogen-bond network appears to enhance the negativity of the $O^{3'}$ atom, as its atomic charge in the LeuRS·valyl-$tRNA^{Leu}$ complex, −0.73, is more negative than the value of −0.63 obtained using a modeled structure of valine-attached A76, isolated from the complex. State 6 is also stabilized by hydrogen bonds between the O atom of the substrate and the second buried water molecule, W_2, and between the O atom and the O^{δ} atom of another threonine, Thr247 (Figure 2a). The negativity of the O atom increases significantly on going from state 1 to state 6, as indicated by decreases in its atomic charge, from −0.54 to −0.63, and the carbonyl group bond order, from 1.73 to 1.31. The above-mentioned hydrogen bonds thus help to stabilize the carbonyl group as it undergoes the changes in its electronic structure that are induced by nucleophilic attack. It is significant that both Thr247 and Thr248 are conserved residues in the aaRSs of various species and that mutations of Thr247 and Thr248, i.e., T247V and T248V, reduce editing activity. Their roles in stabilizing the higher-energy intermediate states along the editing pathway via hydrogen-bonding could provide explanations for these observations.

3.5. Capping Processes for Termination of the Reaction. The editing reaction terminates by cleavage of the $C-O^{2'}$ bond and capping of the $O^{2'}$ atom of the leaving group by a hydrogen atom of the nucleophilic water molecule. To clarify which of the hydrogen atoms, either H_{w1} or H_{w2}, acts to cap the $O^{2'}$ atom, we performed two distinct QM/MM MD simulations using the $O^{2'}-C$ distance and the appropriate $O^{2'}-H_w$ distance as reaction coordinates. The energy barrier for capping by H_{w2} is estimated to be as small as 2.4 kcal/mol (Figure 2a), whereas that for capping by H_{w1} is much higher, at 15.1 kcal/mol (see the Supporting Information, Figure S6). Abstraction of a proton, in this case H_{w2}, from the nucleophile is promoted by the accumulation of negative charge on the $O^{2'}$ atom as the $C-O^{2'}$ bond elongates. In fact, the atomic charge on $O^{2'}$ decreases from −0.48 to −0.56 on going from state 3 to state 6.

The evolution of atomic distances (Figure 2b) and the PES in which the $H_{w2}-O^{2'}$ distance is used as one of the reaction coordinates (Figure 2a) show that decrease in the $H_{w2}-O^{2'}$ distance is counterbalanced by a dramatic increase in the $C-O^{2'}$ distance. After passage of the transition state for proton capping, state 7, this leads to the product state, state 8, in which the $C-O^{2'}$ distance is ∼3.0 Å. The changes in atomic distances show that $H_{w2}-O^{2'}$ bond formation is accompanied by an increase in the $H_{w1}-O^{3'}$ distance, corresponding to breakage of the LBHB between the H_{w1} and $O^{3'}$ atoms in state 7. This is compensated for by the formation of a hydrogen bond between H_{w1} and O^{δ} of Thr247 in state 8. The energies of the various states along

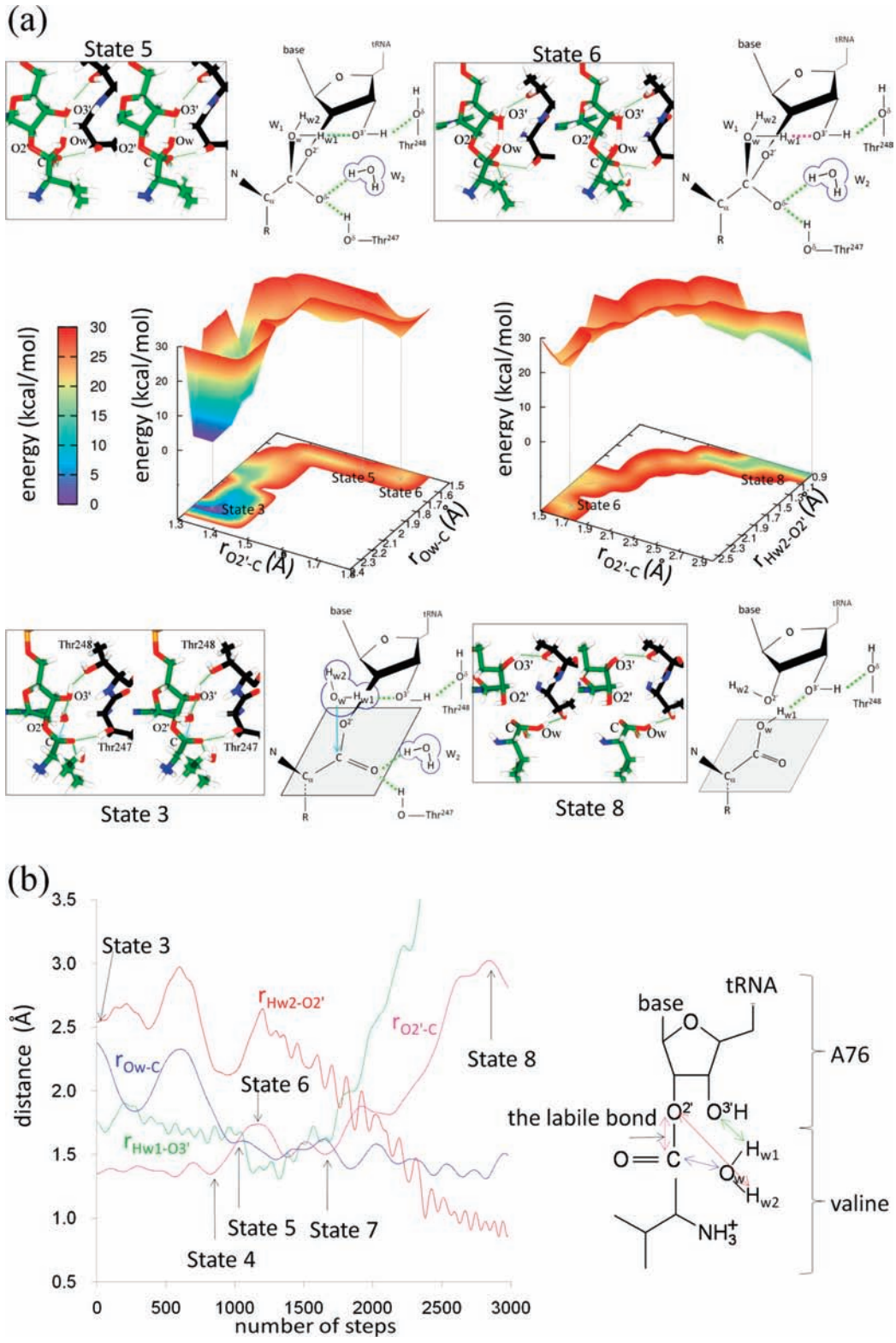

Figure 2. (a) Potential energy surfaces for formation of the O_w-C bond (left panel) and capping of the $O^{2'}$ atom by H_{w1} (right panel) from simulation 3. Vertical and horizontal axes represent the potential energy (kcal/mol) and the reaction coordinates (Å), respectively. Stereoviews and chemical structures of the representative structures corresponding to states 3, 5, 6, and 8 are also shown. (b) Trajectories of the distances r_{Ow-C} (blue), $r_{Hw1-O3'}$ (green), $r_{O2'-C}$ (magenta), and $r_{Hw2-O2'}$ (red) taken from simulation 3.

the pathway obtained by simulation 3 are summarized in Figure 3. State 8 is 10.3 kcal/mol higher in energy than state 3, but release of the products, $tRNA^{Leu}$ and valine, from the catalytic pocket could lead to a further decrease in potential energy.

3.6. Exploration of Reaction Pathways (Part 3). To investigate the plausibility of scheme 2, in which the reaction is initiated by the attack of H_{w1} on $O^{2'}$ (Figure 1e), we performed QM/MM MD simulations using the $H_{w1}-O^{2'}$ and O_w-C

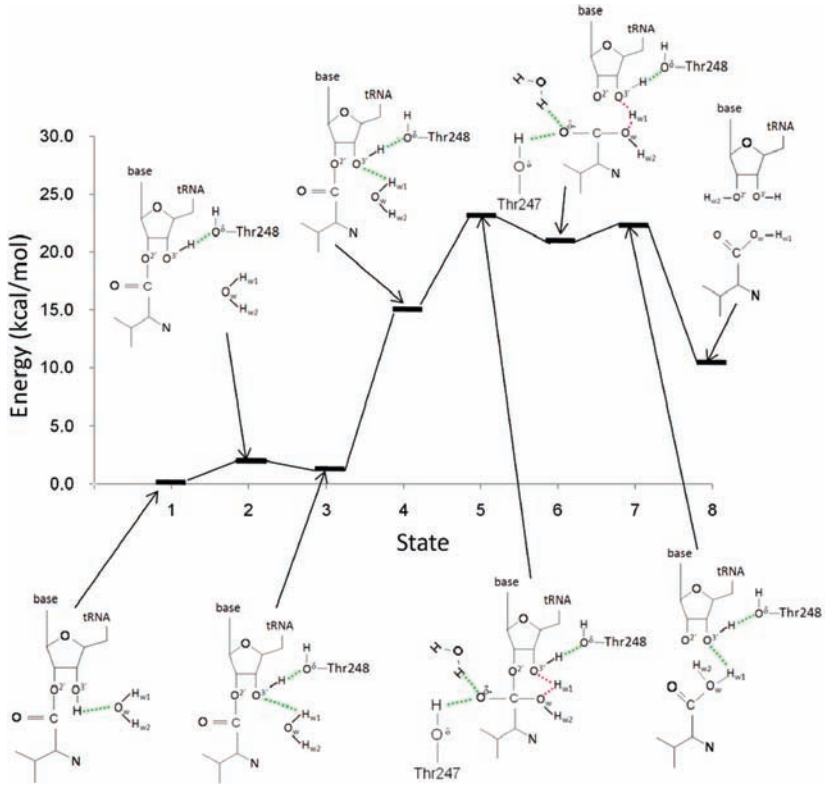

Figure 3. An energy diagram of the editing reaction. The vertical axis represents potential energy (kcal/mol) and the states defined in the text are shown on the horizontal axis. State 1 represents the initial state. In State 2, the dihedral angle, $C^{2'}-C^{3'}-O^{3'}-HO\text{-}3'$, is rotated, resulting in the formation of a hydrogen bond between the O^{δ} atom of Thr248 and H_{w1} and making the carbonyl group of the substrate accessible to nucleophilic water molecules. In state 3, the nucleophile W_1 attacks the carbonyl group. In state 4, W_1 approaches the C atom. In state 5, which corresponds to the transition state, a $C-O_w$ bond is formed along with LBHB between the H_{w1} and $O^{3'}$ atoms. State 6 is a metastable state that is generated by elongation of the $O^{2'}-C$ bond. State 7 represents the transition stage in the transfer of H_{w2} to $O^{3'}$. In state 8, the products are formed.

distances as reaction coordinates (simulation 4). A potential energy of 39.7 kcal/mol was found to be required for abstraction of H_{w1} by $O^{2'}$ atom (see the Supporting Information, Figure S3c,d). The larger energy barrier required for scheme 2, as compared to scheme 1, is due to the fact that $O^{2'}$ has a lower nucleophilicity than O_w, because there are no atoms present to act as the general base for $O^{2'}$, whereas 3′-OH does so for O_w. The significance of choosing the reaction coordinates and employing MD simulation is further discussed in the Supporting Information (sections S2.2 and S2.3).

3.7. The Editing Mechanism Operates by a Ribozyme Reaction. We conclude that post-transfer editing of LeuRS operates by the reaction mechanism described in simulation 3. To validate the result, we recalculated the potential energy barrier in simulation 3 (i.e., the potential energy difference between states 3 and 5) by a higher level ab initio electronic structure method, Møller−Plesset second order perturbation (MP2) theory with the 6-31+G** basis set. The modified value is 26.1 kcal/mol, which is in good agreement with the DFT result, the difference being 2.9 kcal/mol. This shows that possible inaccuracies arising from the DFT method, such as an inadequate description of van der Waals interactions, are significantly smaller than the differences in the energy barriers among the four simulations, confirming our conclusion that simulation 3 is the most feasible pathway.

As further support, biochemical experiments indicate that the 3′-HO of A76 is important for the reaction (see the Supporting Information, section S1), in agreement with our computational results. Thus, in this new scheme, it is $tRNA^{Leu}$, rather than any protein residue, that is responsible for promoting and finalizing the reaction and indicates that the editing reaction is a self-cleavage reaction of the misaminoacylated tRNA. In other words, the misaminoacylated $tRNA^{Leu}$ in complex with LeuRS acts as a ribozyme. The free energy of activation of the self-cleavage reaction in the hammerhead ribozyme has been measured experimentally to be 18.3 kcal/mol,[24] which is comparable to the potential energy barrier calculated here for the LeuRS editing reaction.

3.8. Contribution of the Protein in the Editing Reaction: A Novel Type of Enzyme, "a Hybrid Ribozyme/Protein Catalyst". Although the editing reaction is ribozymal, two conserved threonine residues in the protein, Thr247 and Thr248, contribute to stabilization of the transition state for O_w-C bond formation (state 5) by rotating 3′-HO and by increasing the catalytic power of the $O^{3'}$ atom through formation of a hydrogen-bonding network with the substrate. This means that the ribozymal catalysis is enhanced by the protein moiety, leading us to suggest that LeuRS is an example of a new, hybrid ribozyme/protein category of biomolecular catalyst. To quantify the contribution of the protein, we removed it from the system and calculated the activation barrier via single point energy calculations of the state 3 and 5 structures. The resulting energy barrier is 27.6 kcal/mol, which is 5.6 kcal/mol higher than in the presence of protein. This is consistent with experimental data as a double mutant, Thr247Val/Thr248Val, has a thousand-fold reduction in editing activity, corresponding to an increased activation free-energy barrier of 3.7 kcal/mol (estimated experimentally from changes in k_{cat}/K_M values).[10] The difference

(24) Leclerc, F.; Karplus, M. *J. Phys. Chem. B* **2006**, *110*, 3395–409.

Table 2. Classification of Ribozyme Catalytic Mechanisms

systems	activator[a]	nucleophile	involvement of protein[b]
group I intron	divalent metal ions	2′-OH	×
HDV ribozyme	divalent metal ions	2′-OH	×
hairpin ribozyme	nucleotide bases	2′-OH	×
VS ribozyme	nucleotide bases	2′-OH	×
glmS ribozyme	nucleotide bases	2′-OH	×
hammerhead ribozyme	nucleotide bases	2′-OH	×
peptidyl transferase in ribosome	2′-OH	H_2N-[c]	△
deacylation of peptidyl-CCA in ribosome	2′-OH	H_2O[d]	△
class Ia aaRSs (LeuRS, IleRS, ValRS), class IIa ThrRS,[e] and class IIc PheRS	3′(2′)-OH	H_2O[d]	○

[a] Molecular species to activate nucleophiles. [b] A system marked by ○ (protein moieties contribute to catalysis) or △ (protein moieties do not contribute to catalysis) involves a protein moiety bound to ribozymes, while a system marked by × consists only of RNA molecules.[25,26] [c] The α-amine (H_2N-) of the amino acid moiety of aa-tRNA acts as a nucleophile in the peptidyl-transferase reaction in the ribosome.[27,28] [d] The novel mechanism revealed by the present study in which a water molecule acts as a nucleophile. [e] *P. abyssi* ThrRS.[33]

between the experimental and calculated values (3.7 vs 5.6 kcal/mol) can, in part, be attributed to the stabilizing contribution of other parts of the protein.

3.9. The Editing Mechanism Belongs to a Novel Class of Riboyzme Reaction. Up to now, various ribozyme catalytic mechanisms have been discovered, including self-cleavage reactions in several ribozymes[25,26] and the peptidyl-transferase reaction in ribosomes.[27,28] Such diverse mechanisms have previously been classified as follows (Table 2).[25,26] The group I intron and the hepatitis delta virus (HDV) ribozyme employ a divalent metal as activator of the 2′-OH nucleophile, whereas the hairpin and Varkud satellite (VS) ribozymes exploit nucleotide bases. In ribosomal peptidyl transferase reactions, there is experimental and theoretical evidence that the 2′-OH of A76 of the peptidyl-tRNA bound to the P site (substrate) activates the nucleophile which, in this case, is the α-amino group of the aminoacyl-tRNA bound to the A site.[27–31] In these systems, solvent water molecules are thought to contribute to catalysis by stabilizing intermediate states via hydrogen bonds or by providing hydrogen atoms to cap leaving groups.[32] By contrast, the editing mechanism revealed in the present study provides the first evidence for a novel class of strategies employed by ribozymes in which water is the "leading actor" due to its role as the nucleophile.

3.10. Widespread Occurrence of the Ribozyme Reaction Proposed in the Present Study. With respect to the other class Ia aaRSs, ValRS and IleRS, the substitution of the pertinent OH group of A76 (either 2′ or 3′) with a H atom has a small effect on the editing activity, whereas it has a dramatic effect on the Leu system (see the Supporting Information, Table S1).[11] To explain this difference, we performed further structural modeling of the *T. thermophilus* Val and Ile systems (see the Supporting Information, sections S4.1 and S4.2) and confirmed that, in the wild type enzymes, the major factor activating the nucleophile is indeed the appropriate OH group of A76 of the tRNA. However, when the activating OH group of A76 is removed, its role is compensated for by Asp276 and Glu327 in the Val and Ile systems, respectively. This is not possible in LeuRS, because the equivalent amino acid residue, Asp344, is inactivated, forming a salt bridge with an arginine residue, Arg346 (see the Supporting Information, Figures S8 and S9, section S4.1).

Examination of existing experimental and structural data suggests that other classes of aaRS, such as ThrRS from class IIa and PheRS from class IIc, also exploit the ribozymal catalytic mechanism (see the Supporting Information, Figure S10a and Table S1, sections S4.3 and S4.4).[33–35] In addition, it appears that 3′-OH critically contributes to the deacylation of peptidyl-CCA in the ribosome, the role of which is to release fully synthesized peptide chains (see the Supporting Information, Figure S10b, section S4.5).[36] Thus, this novel class of catalytic mechanism could be of major importance in ribozyme chemistry.

We can divide the ribozyme reactions into two subclasses. In one, protein moieties do not contribute but are simply bound to RNA moieties, whereas in the other protein moieties can have effects on catalysis, as discussed earlier in this report (Table 2). The deacylation of peptidyl-CCA in the ribosome belongs to the former subclass, since none of the protein moieties is close to the catalytic site (see the Supporting Information, Figure S10b, section S4.5). By contrast, the class Ia aaRSs, which possess an editing capability, can be identified as belonging to the second subclass, as discussed earlier. The class II aaRSs that carry out editing, ThrRS and PheRS, may also be members of this subclass. They possess amino acid residues of similar functionality to Thr247 and Thr248 in *T. thermophilus* LeuRS, although the structural identities of the editing domains between class Ia and class IIa/c aaRSs are lost (see the Supporting Information, Figure S10a, section S4.4). Despite these differences, the crystal structure of *P. abyssi* ThrRS in complex with a post-transfer substrate suggests that its editing reaction operates in a similar way to the LeuRS system studied here. This would imply that the functional roles of the protein moieties in the subclass are (i) to position the substrates in the proper conformation for nucleophilic attack, (ii) to provide substrate specificity, and (iii) to promote the tRNA-catalyzed reaction.

3.11. Implications of Hybrid Catalysts for the Molecular Origin of Life. Thus, we have proposed that LeuRS belongs to a category of biomolecular catalyst that we term a hybrid

(25) Cochrane, J. C.; Strobel, S. A. *Acc. Chem. Res.* **2008**, *41*, 1027–35.
(26) Strobel, S. A.; Cochrane, J. C. *Curr. Opin. Chem. Biol.* **2007**, *11*, 636–43.
(27) Schmeing, T. M.; Huang, K. S.; Kitchen, D. E.; Strobel, S. A.; Steitz, T. A. *Mol. Cell* **2005**, *20*, 437–48.
(28) Weinger, J. S.; Parnell, K. M.; Dorner, S.; Green, R.; Strobel, S. A. *Nat. Struct. Mol. Biol.* **2004**, *11*, 1101–6.
(29) Sharma, P. K.; Xiang, Y.; Kato, M.; Warshel, A. *Biochemistry* **2005**, *44*, 11307–14.
(30) Trobro, S.; Aqvist, J. *Proc. Natl. Acad. Sci. U.S.A.* **2005**, *102*, 12395–400.
(31) Trobro, S.; Aqvist, J. *Biochemistry* **2006**, *45*, 7049–56.
(32) Walter, N. G. *Mol. Cell* **2007**, *28*, 923–9.
(33) Hussain, T.; Kruparani, S. P.; Pal, B.; Dock-Bregeon, A. C.; Dwivedi, S.; Shekar, M. R.; Sureshbabu, K.; Sankaranarayanan, R. *EMBO J.* **2006**, *25*, 4152–62.
(34) Kotik-Kogan, O.; Moor, N.; Tworowski, D.; Safro, M. *Structure* **2005**, *13*, 1799–807.
(35) Ling, J.; Roy, H.; Ibba, M. *Proc Natl Acad Sci U S A* **2007**, *104*, 72–7.
(36) Simonovic, M.; Steitz, T. A. *RNA* **2008**, *14*, 2372–8.

ribozyme/protein catalyst. In addition to its intrinsic interest, the existence of such a category has important implications for theories of the molecular origin of life. In the RNA world hypothesis, RNA was the first biologically competent macromolecule. This is supported, for example, by the existence of RNAs that possess the capacity for aminoacylation of tRNAs.[37] Gradually, however, there was a transition to the world that we observe today in which protein and DNA play major roles. The mechanism of the editing reaction revealed in this study provides an example of the type of strategy that could have been important in the switch from ribozymal to enzymic catalysis and provides circumstantial support for the suggestion that contemporary aaRSs were some of the earliest enzymes established during this transition.[38−43]

4. Conclusion

Editing by LeuRS in complex with $tRNA^{Leu}$ attached to an incorrect amino acid is suggested to be a novel ribozymal reaction, in which the protein plays a crucial role in promoting the reaction. This means that editing operates by a "hybrid ribozyme/protein catalyst", which can be categorized as a novel class of enzyme as well as of ribozyme. Analysis of existing experimental data and additional structural modeling imply that editing by other aaRSs and two reactions in the ribosome (peptidyl transfer and deacylation of the peptidyl-CCA moiety) are also members of this novel class of ribozyme, although in the latter case, the protein moieties do not contribute directly to catalysis. Thus, the reaction mechanism identified in this study appears to occur in a number of diverse biological systems.

More specifically, there is biochemical evidence that the other class Ia enzymes - IleRS and ValRS - behave differently to LeuRS with modified tRNAs.[11] However, these apparent discrepancies in the biochemical data can be explained by invoking compensatory reaction pathways that are variants of the wild-type reaction mechanism. Finally, the existence of hybrid ribozyme/protein catalysts, exemplified by the LeuRS editing mechanism, provides insight into the types of transitional forms that could have been important in the RNA world hypothesis for the origin of life.

Acknowledgment. We thank Dr. P. Schimmel for valuable scientific discussions. This work is partly supported by grants-in-aid from the Ministry of Education, Culture, Sports, Science and Technology (MEXT) under contract Nos. 19019003 and 21340108. Computations were performed using computer facilities under the "Interdisciplinary Computational Science Program" at the Center for Computational Sciences, University of Tsukuba, and the Computer Center for Agriculture, Forestry, and Fisheries Research, MAFF, Japan, and the Supercomputer Center, Institute for Solid State Physics, University of Tokyo.

Supporting Information Available: Experimental discrepancy in Ile/Val and Leu systems, further discussions relevant to QM/MM hybrid MD simulations, LBHBs, and other systems which commonly employs the ribozymal reaction mechanism found in this work. This information is available free of charge via the Internet at http://pubs.acs.org.

JA9095208

(37) Illangasekare, M.; Yarus, M. *RNA* **1999**, *5*, 1482–9.
(38) Ribas de Pouplana, L.; Schimmel, P. *Cell. Mol. Life Sci.* **2000**, *57*, 865–70.
(39) Ribas de Pouplana, L.; Schimmel, P. *Trends Biochem. Sci.* **2001**, *26*, 591–6.
(40) Rodin, A. S.; Rodin, S. N.; Carter, C. W., Jr. *J. Mol. Evol.* **2009**, *69*, 555−567.
(41) Rodin, S. N.; Rodin, A. S. *DNA Cell Biol.* **2006**, *25*, 365–75.
(42) Ruan, B.; Ahel, I.; Ambrogelly, A.; Becker, H. D.; Bunjun, S.; Feng, L.; Tumbula-Hansen, D.; Ibba, M.; Korencic, D.; Kobayashi, H.; Jacquin-Becker, C.; Mejlhede, N.; Min, B.; Raczniak, G.; Rinehart, J.; Stathopoulos, C.; Li, T.; Soll, D. *Acta Biochim. Pol.* **2001**, *48*, 313–21.
(43) Schimmel, P.; Ribas de Pouplana, L. *Cell* **1995**, *81*, 983–6.